

Selective control of vortex polarities by microwave field in two robustly synchronized spin-torque nano-oscillators

Yi Li,^{1,*} Xavier de Milly,¹ Olivier Klein,² Vincent Cros,³ Julie Grollier,³ and Grégoire de Loubens^{1,†}

¹*Service de Physique de l'État Condensé, CEA, CNRS, Université Paris-Saclay, Gif-sur-Yvette, France*

²*SPINTEC, Univ. Grenoble Alpes / CEA / CNRS, 38000 Grenoble, France*

³*Unité Mixte de Physique CNRS, Thales, Univ. Paris-Sud, Université Paris-Saclay, Palaiseau, France*

(Dated: March 13, 2022)

Manipulating operation states of coupled spin-torque nano-oscillators (STNOs), including their synchronization, is essential for applications such as complex oscillator networks. In this work we experimentally demonstrate selective control of two coupled vortex STNOs through microwave-assisted switching of their vortex core polarities. First, the two oscillators are shown to synchronize due to dipolar interaction in a broad frequency range tuned by external biasing field. Coherent output is demonstrated along with strong linewidth reduction. Then, we show individual vortex polarity control of each oscillator, which leads to synchronization/desynchronization due to accompanied frequency shift. Our methods can be easily extended to multiple-element coupled oscillator networks.

A growing interest has been witnessed on spin-torque nano-oscillators (STNOs) [1]. They exhibit numerous advantages in applications of modern electronics, such as nano-scale geometry, microwave-frequency signal output and frequency tunability. Particularly, STNOs can be coupled to each other leading to synchronization [2–8]. This provides a platform to study synchronization phenomena [9] as well as to mimic neural networks [10]. A more advanced utilization of STNO networks requires manipulation of synchronization states, or the ability to turn on or off synchronization. To this aim, regular methods include tuning the biasing current and magnetic field in order to vary the output frequencies. However they usually also lead to a modification of the device properties, which thus adds more complexity to the system.

The introduction of vortex-based STNOs [11–13] provides an alternative solution. They have been shown to synchronize efficiently with various coupling mechanisms [5, 6, 8, 14]. With the additional parameter of vortex core polarity, defined as the binary perpendicular direction of the magnetization at the vortex core [15], the sign of the frequency tunability [16] for each STNO can be independently adjusted by dynamically switching the corresponding vortex polarity [17–19], without changing the properties of other devices. This leads to a simple demonstration and control of synchronization [6, 14]. Moreover, the inter-device coupling strength can be also changed from their relative polarity alignments [6, 14, 20], which provides a new method to modify STNO networks.

In this work we explore microwave-assisted vortex polarity switching in a system composed of two dipolarly coupled STNOs. First, by further reducing the inter-device spacing of the two STNOs down to 50 nm compared with our previous work [6], we show their improved synchronization in a broad frequency range with coherent power output and linewidth reduction due to stronger dipolar coupling [21, 22]. Then, we show that in the synchronized state, a microwave field of well chosen fre-

quency and amplitude can selectively switch the vortex polarity of each STNO, leading to two distinct regions of reversal events in the switching portrait. Owing to a nonzero biasing field, the polarity switching is accompanied by a large shift of the auto-oscillation frequency of the corresponding STNO, which results in the turn-off of the synchronization. Furthermore our measurements of the switching portraits in the unsynchronized states yield nearly identical regions for core reversal, which indicates that the switching conditions of two strongly interacting STNOs are mostly insensitive to their coupling. These results provide a new way to control coupled vortex-based STNO arrays.

The sample consists of two adjacent cylindrical spin-valve nanopillars with layer structure of Py(15 nm)/Cu(10 nm)/Py(4 nm) (Py = Ni₈₀Fe₂₀). They have identical nominal diameters of 200 nm and an edge-to-edge separation of 50 nm. An antenna is fabricated on top of the sample to generate an in-plane microwave field h_{rf} . During the experiments the common dc current is set to 41 mA which is twice the critical current for spin transfer induced vortex core auto-oscillation. The auto-oscillation is dominated by the Py(15 nm) layers, whose polarity states will be referred to throughout the paper. The thinner Py layers act as the polarizers [23]. Details of the vortex STNO pair operations can be found elsewhere [6, 14]. A perpendicular biasing field H_B is applied to tune the output frequency [13, 16].

First we demonstrate mutual synchronization of the two STNOs, labeled as 1 and 2. Figs. 1(a-c) show the power spectral density (PSD) as a function of frequency $\omega_{SA}/2\pi$ for various H_B . Three polarity states, $\langle 1 \uparrow 2 \downarrow \rangle$, $\langle 1 \downarrow 2 \uparrow \rangle$ and $\langle 1 \downarrow 2 \downarrow \rangle$, have been studied which are set by microwave-assisted polarity switching as will be discussed later. The $\langle \uparrow \rangle$ (or $\langle \downarrow \rangle$) state is defined as the polarity pointing towards (or away from) the positive H_B direction. For each antiparallel polarity states (Figs. 1a,b), two branches of auto-oscillation signals can be observed,

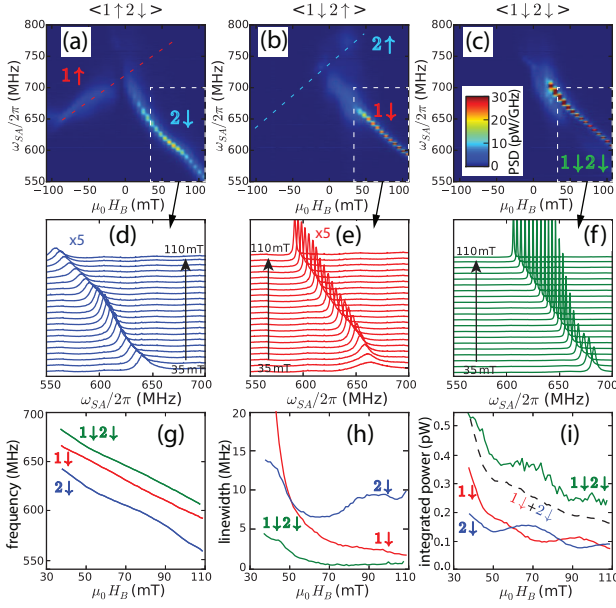


FIG. 1. (a-c) Power spectral densities of (a) $\langle 1 \uparrow 2 \downarrow \rangle$, (b) $\langle 1 \downarrow 2 \uparrow \rangle$ and (c) $\langle 1 \downarrow 2 \downarrow \rangle$ polarity states as a function of $\mu_0 H_B$. (d-f) Zoomed-in spectral lineshapes of (a-c) in the white box regions, from 35 mT to 110 mT. (g-i) Field dependence of (g) frequency, (h) linewidth and (i) integrated powers extracted from (d-f). In (i) the black dashed curve shows the power sum of red and blue curves.

with opposite frequency dependence on H_B due to different polarity alignments to field [16, 24]. We focus on the spectra of $\langle 1 \downarrow \rangle$ and $\langle 2 \downarrow \rangle$ STNOs in the large positive-field region, with the lineshapes plotted in Figs. 1(d-e). Their output frequencies are well separated (> 100 MHz) from their $\langle \uparrow \rangle$ neighbors (see extrapolations of the faint branches in Figs. 1(a) and (b) shown by dashed red and blue lines, respectively). Thus the influence of inter-device dipolar coupling is negligible and the two spectra can be taken as the individual outputs of the STNOs 1 and 2 with $\langle \downarrow \rangle$ polarity states.

Then we move to the parallel polarity state $\langle 1 \downarrow 2 \downarrow \rangle$. Instead of two peaks corresponding to the superposition of the $\langle 1 \downarrow \rangle$ and $\langle 2 \downarrow \rangle$ spectra, only one auto-oscillation peak is observed in Fig. 1(f), with a much stronger amplitude and smaller linewidth in a broad frequency (biasing field) range. The frequencies, full-width half-maximum linewidths and integrated powers are extracted and plotted in Figs. 1(g-i), respectively. For the $\langle 1 \downarrow 2 \downarrow \rangle$ state, the linewidth is greatly reduced from the two individual peaks (Fig. 1h) by more than a factor of two in the entire field range; the output power, plotted with the green curve in Fig. 1(i), is larger than the sum of the two individual devices marked by the black dashed curve. All those evidences show that the two STNOs are mutually synchronized, with coherent output and reduced phase noise. It agrees with our previous observations of mutual synchronization due to dipolar coupling [6, 14].

Next we examine the vulnerability of the synchroniza-

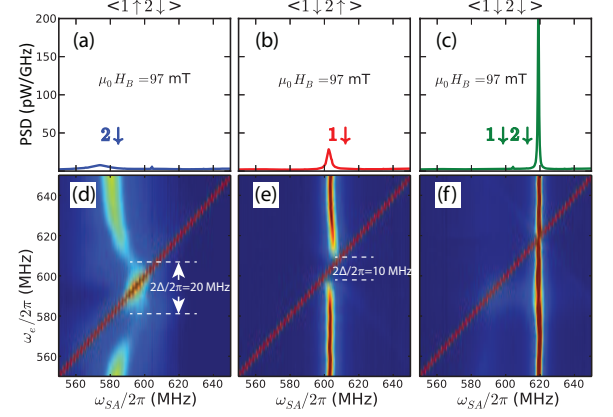


FIG. 2. (a-c) Power spectral densities of (a) $\langle 1 \uparrow 2 \downarrow \rangle$, (b) $\langle 1 \downarrow 2 \uparrow \rangle$ and (c) $\langle 1 \downarrow 2 \downarrow \rangle$ states at $\mu_0 H_B = 97$ mT. (d-f) Power spectral density of (a-c) in the presence of a microwave field ($P_e = -16$ dBm) at various frequencies $\omega_e/2\pi$.

tion state to external perturbation, a weak microwave field in our case. For the three polarity states in Fig. 1, we set the biasing field to $\mu_0 H_B = 97$ mT where clear auto-oscillation spectra can be observed (Figs. 2a-c). Then a microwave power of $P_e = -16$ dBm is applied, which corresponds to a linear amplitude of $\mu_0 h_{rf} = 0.4$ mT. By sweeping its frequency $\omega_e/2\pi$, phase-locking to the microwave field is observed [25, 26] for $\langle 1 \downarrow \rangle$ (Figs. 2d) and $\langle 2 \downarrow \rangle$ (Figs. 2e) peaks with locking bandwidth $\Delta_e/2\pi$ of 10 MHz and 5 MHz, respectively. In contrast, the $\langle 1 \downarrow 2 \downarrow \rangle$ peak is barely influenced by the microwave field and the phase-locking bandwidth is negligible (Fig. 2f). In fact its resilience to the external microwave field is intrinsically connected to the much smaller output linewidth. Owing to the coherent emission, the synchronized two-STNO system is more resistant to environmental noise which is the main source of linewidth broadening [27–29]. The observations in Fig. 2 prove that dipolar-field-induced synchronization can improve the noise stability of STNOs.

In the presence of a strong microwave field, however, the response of synchronization state is completely different from in Fig. 2(f), which provides the opportunity to address the vortex polarities independently. In Fig. 3 we show our main results of microwave-assisted polarity switching for vortex auto-oscillators. This technique has already been demonstrated on a passive vortex [17–19]. For our samples, we firstly set the polarity state to $\langle 1 \downarrow 2 \downarrow \rangle$ state with a strong negative field $\mu_0 H_B = -300$ mT and move to $\mu_0 H_B = 97$ mT, which favors the $\langle \uparrow \rangle$ states. In contract to Fig. 2, a much stronger microwave power P_e is then applied through the antenna for 3 seconds in order to switch the vortex polarity, and the final state is read through its associated emission spectrum (e.g. Figs. 2a-c). Fig. 3(a) shows the switching results

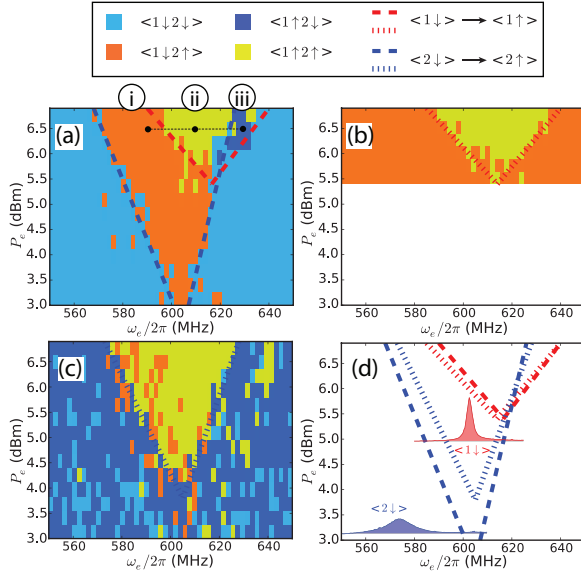


FIG. 3. Microwave switching portraits of vortex polarities for (a) $\langle 1 \downarrow 2 \downarrow \rangle$, (b) $\langle 1 \downarrow 2 \uparrow \rangle$ and (c) $\langle 1 \uparrow 2 \downarrow \rangle$ initial polarity states as demonstrated in Fig. 1(a-c). The bias field is set to $\mu_0 H_B = 97$ mT. The power range is 3.0 to 6.9 dBm in (a), (c) and 5.4 to 6.9 dBm in (b). The power steps are 0.3 dBm and the frequency steps are 2 MHz. The dashed and dotted lines define the boundary of polarity switching events. (d) Switching boundaries plotted in one figure. The blue and red cones correspond to the switching of STNO 1 and 2, respectively. The two lineshapes show the auto-oscillation peaks of $\langle 1 \downarrow \rangle$ and $\langle 2 \downarrow \rangle$, as measured in Fig. 2(a) and (b).

as a function of P_e and $\omega_e/2\pi$. Four different colors represent all possible polarity states. For example, at $P_e = 6.5$ dBm using $\omega_e/2\pi = 590, 610$ and 630 MHz will set the system to (i) $\langle 1 \downarrow 2 \uparrow \rangle$, (ii) $\langle 1 \uparrow 2 \uparrow \rangle$ and (iii) $\langle 1 \uparrow 2 \downarrow \rangle$ final states, respectively. The switching portrait can be categorized into two cone regions whose boundaries are marked by dashed lines: red for flipping $\langle 1 \downarrow \rangle$ to $\langle 1 \uparrow \rangle$ and blue for flipping $\langle 2 \downarrow \rangle$ to $\langle 2 \uparrow \rangle$. The cone-shaped switching boundary agrees well with previous reports on the polarity switching of a passive vortex [19].

To study the relation between the two cone regions and the two STNOs, we repeat the switching experiments for different initial polarity states where oscillators are not synchronized, as $\langle 1 \downarrow 2 \uparrow \rangle$ in Fig. 3(b) and $\langle 1 \uparrow 2 \downarrow \rangle$ in Fig. 3(c). The noise in Fig. 3(c) is mainly due to $\langle 1 \uparrow 2 \downarrow \rangle$ initialization errors. The boundaries of the new switching portraits are depicted by the dotted lines, which are plotted in Fig. 3(d) together with the dashed lines in Fig. 3(a). Due to the absence of synchronization, the switching condition of $\langle 1 \downarrow \rangle$ and $\langle 2 \downarrow \rangle$ should be different from measured in Fig. 3(a). Surprisingly, they coincide pretty well. For comparison the output lineshapes of $\langle 1 \downarrow \rangle$ and $\langle 2 \downarrow \rangle$ are also plotted in Fig. 3(d). The optimal switching frequencies at the bottom of the cone regions are shifted to slightly higher values than the

corresponding auto-oscillation peaks, by 13 MHz for $\langle 1 \downarrow \rangle$ and 29 MHz for $\langle 2 \downarrow \rangle$.

For two interacting vortices, usually their dynamics cannot be disentangled. The polarity states of a coupled vortex pair have been manipulated by resonant microwave excitations, which can only determine the relative polarity state without addressing the state of individual vortices [30–32]. In this scenario, the microwave field acts most effectively at the frequency of the hybridized modes. In the case of two coupled *auto-oscillating* vortices, however, the most effective switching frequency is independent of their mutual synchronization dynamics. Instead the switching pattern in Fig. 3(a) almost equals to the superposition of Figs. 3(b) and (c). The observation can be explained by the different nature of the phase equation for an auto-oscillator, in which the dipolar inter-device coupling *competes* with microwave-oscillator coupling instead of adapting to it. Our experiments indicate that at the threshold of polarity switching, the dipolar coupling is overwhelmed by the stronger microwave coupling. We justify this argument by comparing the two coupling strengths at the switching threshold. For switching powers which are 20 dB larger than those used in Figs. 2(a-b), the microwave coupling strength $\Delta/2\pi$ is in principle ten times greater [26], which is around 50 MHz for STNO 1 and 100 MHz for STNO 2. On the other hand, the dipolar coupling $\Omega/2\pi$ is estimated to be around 10 MHz in the parallel polarity state [14, 20] and is negligible compared with the microwave couplings. The upshift of the optimal switching frequency from the auto-oscillation frequency is due to the nonlinear frequency adjustment as the vortex gyration amplitude increases [33].

Lastly we compare the switching power with the threshold value of a single vortex core. The latter is well understood, where the gyrating vortex core reaches a critical amplitude (velocity) at which its spatial deformation reaches a dynamical instability [34–36]. For Py, the critical velocity [36] is about 320 m/s for a exchange stiffness of 12 pJ/m [37]. At resonance, using the Thiele equation to calculate the gyration amplitude [38], we obtain the vortex core velocity as $v = \gamma \mu_0 h_{rf} R / (3\sqrt{2}\alpha\eta)$, where $R = 100$ nm is the radius of the nanodisc, α is the Gilbert damping of Py, and $\eta \sim 1.7$ is the topological renormalization of the damping [33]. The factor $\sqrt{2}$ accounts for that the microwave field is linearly polarized. Using $\alpha = 0.008$ for Py, the critical microwave field for vortex polarity switching is $\mu_0 h_{rf} \sim 1$ mT, which is around 2 dBm for the geometry of our antenna. The measurements in Fig. 3 yield similar switching powers for STNOs 1 and 2, which indicates that the injected dc current and corresponding spin transfer torque do not essentially change the behavior of a single vortex at large microwave drives.

In summary, we have experimentally demonstrated coherent and robust synchronization of two vortex STNOs

coupled by their dipolar interaction in a broad frequency range. Their synchronization state can be controlled by microwave-assisted vortex polarity switching. We highlight this device-selective, coupling-insensitive and channel-sharing polarity switching technique, which is a technical requirement in small and densely packed STNO networks. We also note that energy-efficient switching is possible with microwave pulses [17, 19] for the operation of such networks. Our results add new understanding to the interacting mechanism of a strong microwave to two coupled auto-oscillators and provide new potential to dipolarly-coupled vortex STNOs for the implementation of coupled oscillator networks. We thank S. Giraud and C. Deranlot for their helps on sample growth and nanofabrication. We acknowledge the MEMOS project ANR-14-CE26-0021 and the MOSAIC project ICT-FP7 317950 for financial support.

* yi.li@cea.fr

† gregoire.deloubens@cea.fr

- [1] S. I. Kiselev, J. C. Sankey, I. N. Krivorotov, N. C. Emley, R. J. Schoelkopf, R. A. Buhrman, and D. C. Ralph, "Microwave oscillations of a nanomagnet driven by a spin-polarized current," *Nature*, vol. 425, p. 380, 2003.
- [2] S. Kaka, M. R. Pufall, W. H. Rippard, T. J. Silva, S. E. Russek, and J. A. Katine, "Mutual phase-locking of microwave spin torque nano-oscillators," *Nature*, vol. 437, p. 389, 2005.
- [3] F. B. Mancoff, N. D. Rizzo, B. N. Engel, and S. Tehrani, "Phase-locking in double-point-contact spin-transfer devices," *Nature*, vol. 437, p. 393, 2005.
- [4] A. Ruotolo, V. Cros, B. Georges, A. Dussaux, J. Grollier, C. Deranlot, R. Guillemet, K. Bouzehouane, S. Fusil, and A. Fert, "Phase-locking of magnetic vortices mediated by antivortices," *Nature Nano.*, vol. 4, p. 528, 2009.
- [5] S. Sani, J. Persson, S. M. Mohseni, Y. Pogoryelov, P. K. Muduli, A. Eklund, G. Malm, M. Käll, A. Dmitriev, and J. Åkerman, "Mutually synchronized bottom-up multi-nanocontact spin-torque oscillators," *Nat. Commun.*, vol. 4, p. 2731, 2013.
- [6] N. Locatelli, A. Hamadeh, F. Abreu Araujo, A. D. Belanovsky, P. N. Skirdkov, R. Lebrun, V. V. Naletov, K. A. Zvezdin, M. Muñoz, J. Grollier, O. Klein, V. Cros, and G. de Loubens, "Efficient synchronization of dipolarly coupled vortex-based spin transfer nano-oscillators," *Sci. Rep.*, vol. 5, p. 17039, 2015.
- [7] A. Houshang, E. Iacocca, P. Dürrenfeld, S. R. Sani, J. Åkerman, and R. K. Dumas, "Spin-wave-beam driven synchronization of nanocontact spin-torque oscillators," *Nat. Nano.*, vol. 11, p. 280, 2015.
- [8] R. Lebrun, S. Tsunegi, P. Bortolotti, H. Kubota, A. S. Jenkins, M. Romera, K. Yakushiji, A. Fukushima, J. Grollier, S. Yuasa, and V. Cros, "Mutual synchronization of spin torque nano-oscillators through a non-local and tunable electrical coupling," *Nat. Commun.*, vol. 8, p. 15825, 2017.
- [9] A. Pikovsky, M. Rosenblum, and J. Kurths, *Synchronization: A universal concept in nonlinear sciences*. Cambridge University Press, Cambridge, UK, 2001.
- [10] J. Grollier, D. Querlioz, and M. D. Stiles, "Spintronic nanodevices for bioinspired computing," *Proc. IEEE*, vol. 104, p. 2024, 2016.
- [11] V. S. Pribiag, I. N. Krivorotov, G. D. Fuchs, P. M. Braganca, O. Ozatay, J. C. Sankey, D. C. Ralph, and R. A. Buhrman, "Magnetic vortex oscillator driven by d.c. spin-polarized current," *Nature Phys.*, vol. 3, p. 498, 2007.
- [12] A. Dussaux, B. Georges, J. Grollier, V. Cros, A. V. Khvalkovskiy, A. Fukushima, M. Konoto, H. Kubota, K. Yakushiji, S. Yuasa, K. A. Zvezdin, K. Ando, and A. Fert, "Large microwave generation from current-driven magnetic vortex oscillators in magnetic tunnel junctions," *Nat. Commun.*, vol. 1, p. 8, 2010.
- [13] N. Locatelli, V. V. Naletov, J. Grollier, G. de Loubens, V. Cros, C. Deranlot, C. Ulysse, G. Faini, O. Klein, and A. Fert, "Dynamics of two coupled vortices in a spin valve nanopillar excited by spin transfer torque," *Appl. Phys. Lett.*, vol. 98, p. 062501, 2011.
- [14] Y. Li, X. de Milly, F. Abreu Araujo, O. Klein, V. Cros, J. Grollier, and G. de Loubens, "Probing phase coupling between two spin-torque nano-oscillators with an external source," *Phys. Rev. Lett.*, vol. 118, p. 247202, Jun 2017.
- [15] T. Shinjo, T. Okuno, R. Hassdorf, K. Shigeto, and T. Ono, "Magnetic vortex core observation in circular dots of permalloy," *Science*, vol. 289, p. 930, 2000.
- [16] G. de Loubens, A. Riegler, B. Pigeau, F. Lochner, F. Boust, K. Y. Guslienko, H. Hurdequint, L. W. Molenkamp, G. Schmidt, A. N. Slavin, V. S. Tiberkevich, N. Vukadinovic, and O. Klein, "Bistability of vortex core dynamics in a single perpendicularly magnetized nanodisk," *Phys. Rev. Lett.*, vol. 102, p. 177602, 2009.
- [17] B. Van Waeyenberge, A. Puzic, H. Stoll, K. W. Chou, T. Tylliszczak, H. R., M. Fähnle, H. Brückl, K. . Rott, G. Reiss, I. Neudecker, D. Weiss, C. H. Back, and G. Schütz, "Magnetic vortex core reversal by excitation with short bursts of an alternating field," *Nature*, vol. 444, p. 461, 2006.
- [18] K. Yamada, S. Kasai, Y. Nakatani, K. Kobayashi, H. Kohno, A. Thiaville, and T. Ono, "Electrical switching of the vortex core in a magnetic disk," *Nature Mater.*, vol. 6, p. 270, 2007.
- [19] B. Pigeau, G. de Loubens, O. Klein, A. Riegler, F. Lochner, G. Schmidt, and L. W. Molenkamp, "Optimal control of vortex-core polarity by resonant microwave pulses," *Nature Phys.*, vol. 7, p. 26, 2011.
- [20] F. Abreu Araujo, A. D. Belanovsky, P. N. Skirdkov, K. A. Zvezdin, A. K. Zvezdin, N. Locatelli, R. Lebrun, J. Grollier, V. Cros, G. de Loubens, and O. Klein, "Optimizing magnetodipolar interactions for synchronizing vortex based spin-torque nano-oscillators," *Phys. Rev. B*, vol. 92, p. 045419, 2015.
- [21] A. D. Belanovsky, N. Locatelli, P. N. Skirdkov, F. Abreu Araujo, J. Grollier, K. A. Zvezdin, V. Cros, and A. K. Zvezdin, "Phase locking dynamics of dipolarly coupled vortex-based spin transfer oscillators," *Phys. Rev. B*, vol. 85, p. 100409(R), 2012.
- [22] A. D. Belanovsky, N. Locatelli, P. N. Skirdkov, F. Abreu Araujo, K. A. Zvezdin, J. Grollier, V. Cros, and A. K. Zvezdin, "Numerical and analytical investigation of the synchronization of dipolarly coupled vortex spin-torque nano-oscillators," *Appl. Phys. Lett.*, vol. 103,

- p. 122405, 2013.
- [23] A. V. Khvalkovskiy, J. Grollier, N. Locatelli, Y. V. Gorbunov, K. A. Zvezdin, and V. Cros, “Nonuniformity of a planar polarizer for spin-transfer-induced vortex oscillations at zero field,” *Appl. Phys. Lett.*, vol. 96, p. 212507, 2010.
 - [24] A. S. Jenkins, E. Grimaldi, P. Bortolotti, R. Lebrun, H. Kubota, K. Yakushiji, A. Fukushima, G. de Loubens, O. Klein, S. Yuasa, and V. Cros, “Controlling the chirality and polarity of vortices in magnetic tunnel junctions,” *Appl. Phys. Lett.*, vol. 105, p. 172403, 2014.
 - [25] W. H. Rippard, M. R. Pufall, S. Kaka, T. J. Silva, S. E. Russek, and J. A. Katine, “Injection locking and phase control of spin transfer nano-oscillators,” *Phys. Rev. Lett.*, vol. 95, p. 067203, 2005.
 - [26] A. Hamadeh, N. Locatelli, V. V. Naletov, R. Lebrun, G. de Loubens, J. Grollier, O. Klein, and V. Cros, “Perfect and robust phase-locking of a spin transfer vortex nano-oscillator to an external microwave source,” *Appl. Phys. Lett.*, vol. 104, p. 022408, 2014.
 - [27] J.-V. Kim, V. Tiberkevich, and A. N. Slavin, “Generation linewidth of an auto-oscillator with a nonlinear frequency shift: Spin-torque nano-oscillator,” *Phys. Rev. Lett.*, vol. 100, p. 017207, Jan 2008.
 - [28] B. Georges, J. Grollier, M. Darques, V. Cros, C. Deranlot, B. Marcilhac, G. Faini, and A. Fert, “Coupling efficiency for phase locking of a spin transfer nano-oscillator to a microwave current,” *Phys. Rev. Lett.*, vol. 101, p. 017201, Jul 2008.
 - [29] A. Slavin and V. Tiberkevich, “Nonlinear auto-oscillator theory of microwave generation by spin-polarized current,” *IEEE Trans. Magn.*, vol. 45, p. 1875, 2009.
 - [30] S. Jain, V. Novosad, F. Fradin, J. Pearson, V. Tiberkevich, A. Slavin, and S. Bader, “From chaos to selective ordering of vortex cores in interacting mesomagnets,” *Nat. Commun.*, vol. 3, p. 1330, 2012.
 - [31] S. Jain, V. Novosad, F. Y. Fradin, J. E. Pearson, and S. D. Bader, “Dynamics of coupled vortices in perpendicular field,” *Appl. Phys. Lett.*, vol. 104, p. 082409, 2014.
 - [32] M. Hanze, C. F. Adolff, B. Schulte, J. Moller, M. Weigand, and G. Meier, “Collective modes in three-dimensional magnonic vortex crystals,” *Sci. Rep.*, vol. 6, p. 22402, 2016.
 - [33] A. Dussaux, A. V. Khvalkovskiy, P. Bortolotti, J. Grollier, V. Cros, and A. Fert, “Field dependence of spin-transfer-induced vortex dynamics in the nonlinear regime,” *Phys. Rev. B*, vol. 86, p. 014402, 2012.
 - [34] R. Hertel, S. Gliga, M. Fahnle, and C. M. Schneider, “Ultrafast nanomagnetic toggle switching of vortex cores,” *Phys. Rev. Lett.*, vol. 98, p. 117201, 2007.
 - [35] K. Y. Guslienko, K.-S. Lee, and S.-K. Kim, “Dynamic origin of vortex core switching in soft magnetic nanodots,” *Phys. Rev. Lett.*, vol. 100, p. 027203, Jan 2008.
 - [36] K.-S. Lee, S.-K. Kim, Y.-S. Yu, Y.-S. Choi, K. Y. Guslienko, H. Jung, and P. Fischer, “Universal criterion and phase diagram for switching a magnetic vortex core in soft magnetic nanodots,” *Phys. Rev. Lett.*, vol. 101, p. 267206, Dec 2008.
 - [37] Y. Li and W. E. Bailey, “Wave-number-dependent gilbert damping in metallic ferromagnets,” *Phys. Rev. Lett.*, vol. 116, p. 117602, Mar 2016.
 - [38] K. Y. Guslienko, “Low-frequency vortex dynamic susceptibility and relaxation in mesoscopic ferromagnetic dots,” *Appl. Phys. Lett.*, vol. 89, p. 022510, 2006.